Fracture Toughness of a Hybrid Rubber Modified Epoxy. II. Effect of Loading Rate

M. Abadyan,[1] M. A. Kouchakzadeh,[1] R. Bagheri[2]

[1]*Engineering Department, Shahrekord Branch, Islamic Azad University, Shahrekord, Iran*
[2]*Department of Materials Science & Engineering, Sharif University of Technology, Tehran, Iran*

Received 9 December 2008; accepted 29 July 2011
DOI 10.1002/app.35379
Published online 27 January 2012 in Wiley Online Library (wileyonlinelibrary.com).

ABSTRACT: Effect of loading rate on toughness characteristics of hybrid rubber-modified epoxy was investigated. Epoxy was modified by amine-terminated butadiene acrylonitrile (ATBN) and recycled tire. Samples were tested at various loading rates of 1–1000 mm/min. Fracture toughness measurements revealed synergistic toughening in hybrid system at low loading rates (1–10 mm/min); hybrid system exhibited higher fracture toughness value in comparison with the ATBN-modified resin with same modifier content. However, synergistic toughening was eliminated by increasing the loading rate. At higher loading rates (10–1000), the fracture toughness of hybrid system decreased gradually to the level lower than that of ATBN-modified epoxy. Fractography of the damage zones showed the toughening mechanisms of ATBN-modified system was less affected by increasing the loading rate compared to that of hybrid system. © 2012 Wiley Periodicals, Inc. J Appl Polym Sci 125: 2476–2483, 2012

Key words: epoxy resin; rubber toughening; hybrid compound; loading rate; fracture toughness

INTRODUCTION

Rubber modification can successfully increase fracture toughness of brittle epoxies via facilitating plastic deformation of the matrix.[1–7] The use of two types of rubber particles might lead to hybrid epoxies with enhanced values of crack resistance.[8–11] If the toughening mechanisms interact in a positive manner, a synergistic toughening may be achieved in which, the fracture toughness of hybrid system is greater than that of an epoxy modified with a single rubber modifier.[9–11] Chen and Jan[9] found that the fracture toughness of an epoxy containing both coarse and fine rubber particles was higher than that of the epoxy containing either of the two modifiers. Bagheri et al.[10] also reported synergistic toughening in an epoxy modified with two different sizes of rubber particles. These investigators claimed that plastic zone branching is responsible for the synergism observed. An earlier work in this group revealed that branching of the crack tip can also results in synergistic toughening in a rubber toughened epoxy containing bimodal size particles.[11]

On the other hand, due to the nature of polymeric materials, their mechanical properties are very much rate-dependent. Some researcher have examined the influence of strain are on toughening of rubber-modified epoxies.[12–14] Low and Mai[12] studied the failure mechanisms of modified epoxies over a wide range of strain rates. They found that the critical strain energy release rate of rubber-modified epoxy decreases with increasing the strain rate. Du et al.,[13] studied the fracture behavior of a rubber-modified epoxy at various loading rates. These investigators observed that the toughening mechanisms were suppressed at high strain rates.

Despite the synergistic toughening observed in rubber-modified epoxies containing bimodal size particles, no investigation has been performed on the influence of strain rate on synergism in such systems. Therefore, the goal of the current study is to examine the concept of synergistic toughening in terms of the rate dependency in bimodal size rubber modified epoxies. The epoxy system used in this study is the same as that of the previous study.[11] In previous work, synergistic toughening were observed in a special formulation and the toughening mechanisms of hybrid modified epoxy were explained in detail. The loading rate, however, is varied in a wide range. It is expected that the results of this study further clarify the applicability of the concept of synergistic toughening in rubber-modified epoxies.

EXPERIMENTS

Materials

The epoxy (Araldite LY564) used is a Diglycidyle Ether of Bisphenol A (DGEBA) system with an epoxy equivalent weight of 170 g/eq from Hauntsman

Correspondence to: R. Bagheri (rezabagh@sharif.edu).

TABLE I
Formulations Made in This Study

LY564 (g)	HY2962 (g)	Tire content (phr)	ATBN content (phr)	Designation
100	25	0	0	NEAT
100	25	0	10	A10
100	25	2.5	7.5	A*10

cured with a cycloaliphatic polyamine hardener (HY2962) from Vantico, Switzerland. Two types of rubber modifiers used in this study; ATBN reactive oligomer (Hycar1300 × 16) with 16% acrylonitrile, molecular weight of 3600 and amine equivalent weight of 900 from Noveon Inc., USA and ground recycled rubber particles, named Tire for simplicity, from Dena, Iran, with mean particle size of 150 μm.

Processing

The epoxy resin and 25 phr hardener were mixed and degassed at room temperature for about 20 min. The mixture was poured into a 5-mm-thick glass mold that had been preheated at 90°C. Curing was performed at 90°C for 6 h in a circulating air oven. Specimens were cut from the plaques prepared by this procedure. In single-modifier formulations, modifier and epoxy were mixed at room temperature under vacuum for 30 min before adding the curing agent. In the case of hybrid systems, ATBN was mixed for 30 min with epoxy prior to adding Tire particles. The blend was then mixed for 10 min before addition of curing agent. The designation for each material prepared is shown in Table I.

Characterization techniques

Tensile properties of resin were determined according to ASTM D638 at cross-head speeds in the range of 5–500 mm/min. Fracture tests were performed using 5-mm thick single-edge-notch (SEN) specimens tested in three-point-bending (3PB) geometry according to ASTM D5045 guideline. Sharp precracks were introduced at notch tips by tapping on a new razor blade chilled in liquid nitrogen. To study the effect of loading rate on fracture behavior of resins, tests were performed at cross-head speeds in the range of 1–1000 mm/min. The following relations were used to calculate plane strain fracture toughness, K_{IC}:

$$K_{IC} = \frac{Ps}{tw^{3/2}} f(a/w) \tag{1}$$

$$f(X) = \frac{3X^{1/2}[1.99 - X(1-X)(2.15 - 3.93X + 2.7X^2)]}{2(1+2X)(1-X)^{3/2}} \tag{2}$$

where P is the maximum load at the instance of crack initiation, t is the thickness of the specimen, s is the span width, w is the width of the specimen, a is the initial crack length, and $f(X)$ is the nondimensional shape factor where X is the same as a/w ($X = a/w$). To ensure plane strain and avoid excessive plasticity, it is required that the size criterion be satisfied according to the following:

$$t, a, (w-a) > 2.5(K_{IC}/\sigma_y)^2 \tag{3}$$

where σ_y is the yield strength of material.

The strain energy release rate, G_{IC}, was calculated from K_{IC} and Young's modulus; E, using the expression for plane strain conditions:

$$G_{IC} = \frac{(1-v^2)K_{IC}^2}{E} \tag{4}$$

where $v = 0.36$, is Poisson's ratio of the material that was estimated using a rule of mixtures, $v = \Sigma V_i v_i$, where V_i and v_i are the volume fraction and the Poisson's ratio of component i, i.e., 0.35 for epoxy-amine and 0.5 for rubber.

All reported values are the average of five independent measurements.

Fractography

To study the structure of crack tip damage zone of specimens, double-notched-four point bending (DN-4PB) method is employed. Details of this technique are as follows: first two edge cracks of equal length were introduced to a bending sample (Fig. 1). The specimen is loaded in a four-point bending fixture at cross-head speeds of 5, 50, and 500 mm/min, until damage zones form at the crack tips. Finally, one of the cracks, which first reach to the instability point, propagates and sample fractures. The other crack that is unloaded contains a well-developed damage zone, and represents the conditions prior to the failure of the material. The fracture surfaces of the broken specimens were observed using scanning electron microscopy (SEM) at an accelerating voltage of 20 kV. The other crack which was unloaded,

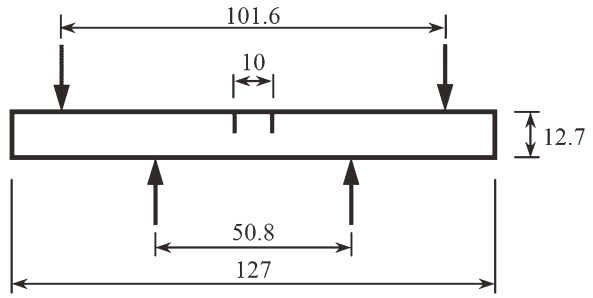

Figure 1 Schematic of DN-4PB specimens used for observation of the crack tip damage zone. All dimensions are in mm.

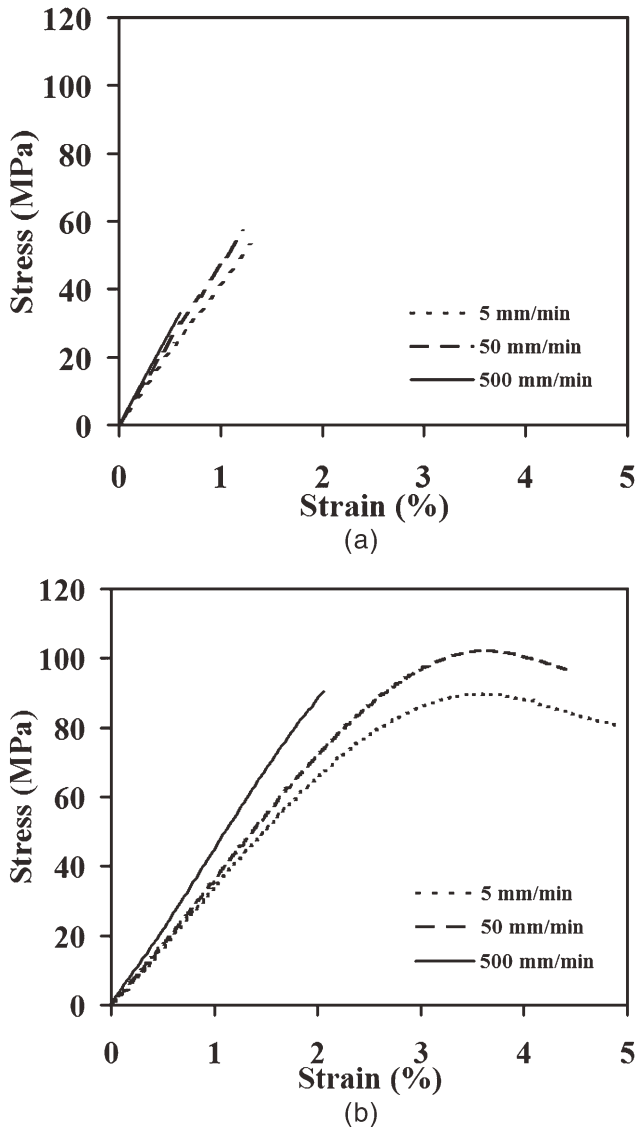

Figure 2 Stress versus strain curve for (a): A*10 and (b): A10 at loading rates of: 5, 50 and 500 mm/min.

therefore, contained a well-developed damage zone that represented the conditions prior to the failure of the material. This damage zone could be observed using transmission optical microscopy (TOM) after polishing the specimen to the thickness of about 150 μm.

RESULTS

Tensile properties

To study the effect of loading rate on tensile properties of A10 and A*10 specimens, tensile tests were performed at crosshead speeds of 5, 50, and 500 mm/min. The results are shown in Figure 2 and illustrate that increasing in loading rate leads to increasing in modulus and decreasing in elongation to failure. This figure also reveals that while the fracture strength does not have a significant dependence to the loading rate in A10, in the hybrid blend, a dramatic influence of the loading rate on the fracture strength is observed. As seen in Figure 2, while A10 shows a relatively ductile behavior, especially at low strain rates, A*10 behaves brittle at all loading rates.

Toughness measurements

Fracture toughness of specimens were measured under a range of applied loading rate of 1–1000 mm/min. Figure 3(a,b) show the fracture toughness (K_{IC}) and strain energy release rate (G_{IC}) results obtained, respectively. The plane strain condition is achieved attending dimensions and mechanical characteristics of the samples. As seen, the toughness of all samples decreases by increasing the loading rate. In addition, Figure 3 illustrates a sharper dependence of toughness to the loading rate in the case of

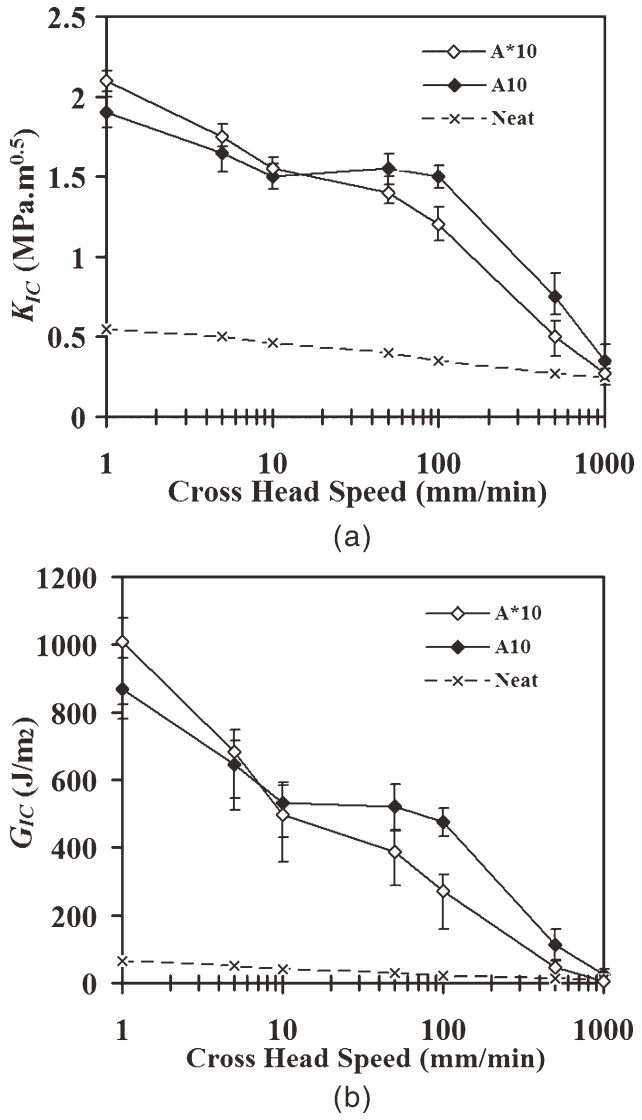

Figure 3 Effect of loading rate on the fracture toughness of samples: (a) K_{IC}, (b) G_{IC}.

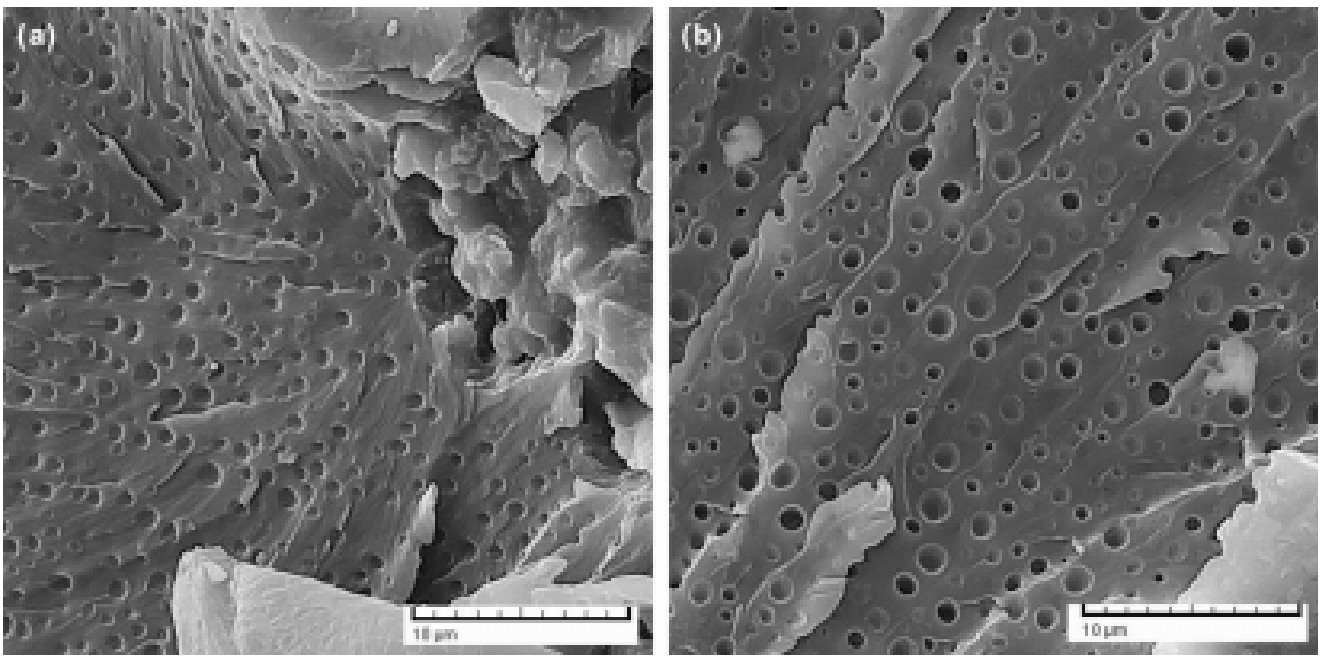

Figure 4 SEM photos taken from the damage surface of samples were tested at 5 mm/min: (a) A*10, (b) A*10 at higher magnification, (c) A10, (d) A10 at higher magnification.

epoxy blends, i.e., A10 and A*10 samples, compared to the neat epoxy. This observation is consistent with that of Du et al.,[13] who attributed the higher strain rate dependency of fracture toughness of the rubber modified epoxy to the strain rate sensitivity of the toughening mechanisms.

On the basis of the tensile results presented in Figure 2, one may expect a much more ductile behavior and thus, a higher fracture toughness[15] in the case of A10 compared to A*10. However, Figure 3 illustrates a higher fracture toughness in the case of A*10 at low loading rates. Considering the different toughening mechanisms of the two systems presented in the earlier work,[11] it is not so strange that the tougher material, i.e., A*10, behaves more brittle in the tensile test. It is note worthy, that the earlier study revealed crack branching as the source of synergistic toughening in A*10, while shear yielding is the active toughening mechanism in A10.

Surprisingly, Figure 3 also illustrates a more sensitivity of K_{IC} to the loading rate in the A*10 compared to the A10. In other words, while A*10 has higher fracture toughness than A10 at low strain rates due to synergistic toughening,[11] it behaves more brittle at higher strain rates. As seen in the figure, no synergistic toughening exists at loading rates equal or greater than 50 mm/min since A10 has larger fracture toughness values than A*10 at this loading range. It is note worthy, that at the very high loading rate of 1000 mm/min, there is negligible difference in fracture toughness values of the neat epoxy and the modified blends (Fig. 3). A similar result was reported by Du et al.,[13] in a CTBN modified epoxy.

To analyze the fracture toughness results obtained and especially, to elucidate the influence of the loading rate on crack growth resistance, more investigations including microscopic evaluations have been incorporated.

Microscopic analyses

Loading rate of 5 mm/min

Figure 4 depicts the SEM micrographs which are taken from the damage zone of specimens at the loading rate of 5 mm/min. Figure 4(a,b) show the fracture surface of A10 and A*10 specimens, respectively. Cavitated ATBN particles are observed in both figures. The magnitude of cavitation and void growth can be determined by means of SEM micrographs. Using image-analysis technique, it is found that the volume fraction of cavities in Figure 4(a,b) are ¯12 and 19%, respectively. Considering the total rubber content of 10 vol % in both materials, it comes that the extent of cavitation of ATBN particles in A*10 and A10 is about 50 and 80%, respectively, (Please note that the original ATBN content in A*10 is less than 8 vol %).

TOM micrographs taken from the crack tip damage zones of A*10 and A10 at loading rate of 5 mm/min are shown in Figure 5. This Figure shows major difference between toughening mechanisms of A*10 and A10. Figure 5 reveals that massive crack

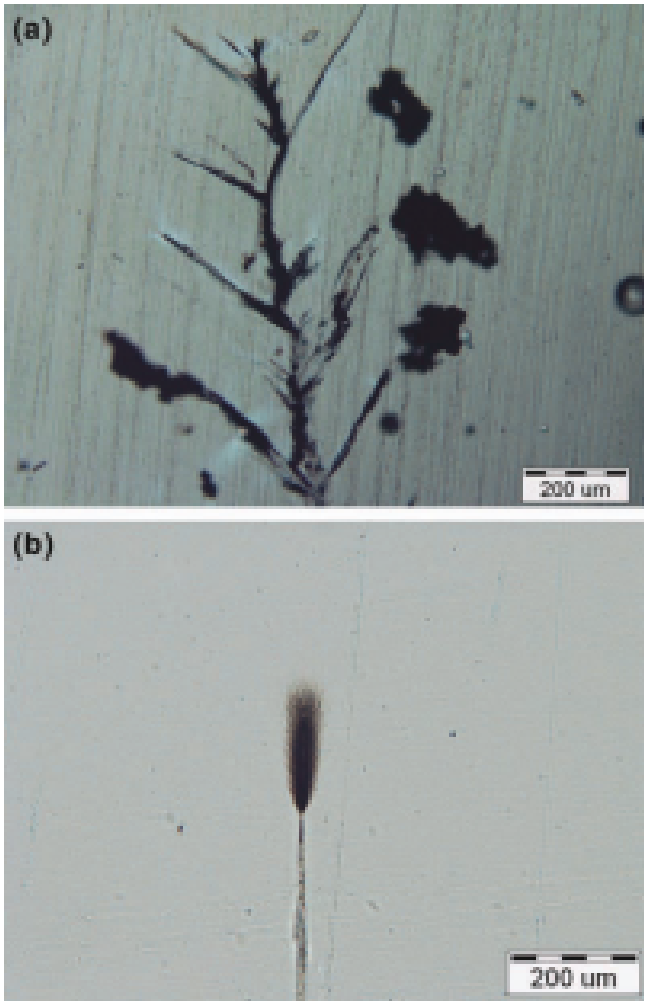

Figure 5 TOM photos of the midplane of the crack tip damage zone of samples tested at 5 mm/min: (a) A*10, (b) A10. [Color figure can be viewed in the online issue, which is available at wileyonlinelibrary.com].

branching and shear yielding are the dominant toughening mechanism for A*10 and A10, respectively. As it has been discussed in previous work, fine ATBN particles increase toughness by increasing the size of the damage zone and respective plastic deformation in the vicinity of the crack tip.[11] However, in the case of hybrid resin (A*10), coarse recycled rubber particles acted as large stress concentrators and resulted in branching of the original crack tip. Mode mixity at the branch tips led to synergistic fracture toughness in hybrid system.[11]

Loading rate of 50 mm/min

Figure 6 shows the SEM micrographs taken from the damage zone of specimens at the loading rate of 50 mm/min. Figure 6(a) illustrates the fracture surface of A*10. Examination of the extent of cavitation by increasing the loading rate in A*10 shows less cavitation at the loading rate of 50 mm/min [comparing Figs. 4(a) and 6(a)]. It is noteworthy, that the extent of cavitation in Figure 6(a) is ~12%. Figure 6(b) shows the fracture surface of A (10) specimen. The measured value of the degree of cavitation in Figure 6(b) is about 53% which is significantly higher than that of A*10 [Fig. 6(a)]. This observation is parallel to the lower toughness of the specimen tested at higher loading rate (Fig. 3).

TOM micrographs taken from the crack tip damage zone of samples at loading rate of 50 mm/min are shown in Figure 7. As seen, crack branching of A*10 decreases significantly by increasing the loading rate [compare Figs. 5(a) and 7(a)]. This may explain the drop in toughness of A*10 at 50 mm/min loading rate compared to that of 5 mm/min (Fig. 3). On the other hand, comparing Figures 5(b) and 7(b) reveals almost identical crack tip plastic zone sizes in A10 at two loading rates of 5 and 50 mm/min. Observation of comprehensive plastic deformation at the crack tip in Figure 7(b) could be explained by the fact that yielding phenomenon is observed in tensile test of A10 at the loading rate of 50 mm/min [Fig. 2(b)]. This may explicate why Figure 3 illustrates almost identical toughness values in A10 tested at the mentioned loading rates.

Recalling the fact observed in Figure 3 that no synergistic toughening occurs at loading rates equal or greater than 50 mm/min, can be attributed to the observations made in Figures 5 and 7. Please note that the crack branching which is responsible for toughening of A*10 is suppressed by increasing the loading rate from 5 to 50 mm/min [compare Figs. 5(a) and 7(a)]. While crack tip shear yielding that is the dominant toughening mechanism of A10, is not diminished by increasing the loading range within the mentioned range [compare Figs. 5(b) and 7(b)]. In other words, the crack branching is more sensitive to one order of magnitude increase in loading rate (from 5 to 50 mm/min) than the shear yielding mechanism. Therefore, the fracture behavior of A*10 is more sensitive than A10 to the variations of the loading rate.

Loading rate of 500 mm/min

Figure 8 shows SEM micrographs of fracture surfaces of modified blends at loading rate of 500 mm/min. As this Figure illustrates, particle cavitation and void growth is suppressed at high loading rate.

Figure 9 shows TOM micrographs taken from the crack tip damage zone of A10 and A*10 at loading rate of 500 mm/min. As Figure 9(a) shows, no toughening mechanism i.e., crack branching or deflection, is observed at the crack tip of A*10. Lack of any crack resistance mechanism explains why toughness of A*10 is near to that of NEAT sample at very high loading rate of 500 mm/min (Fig. 3). The

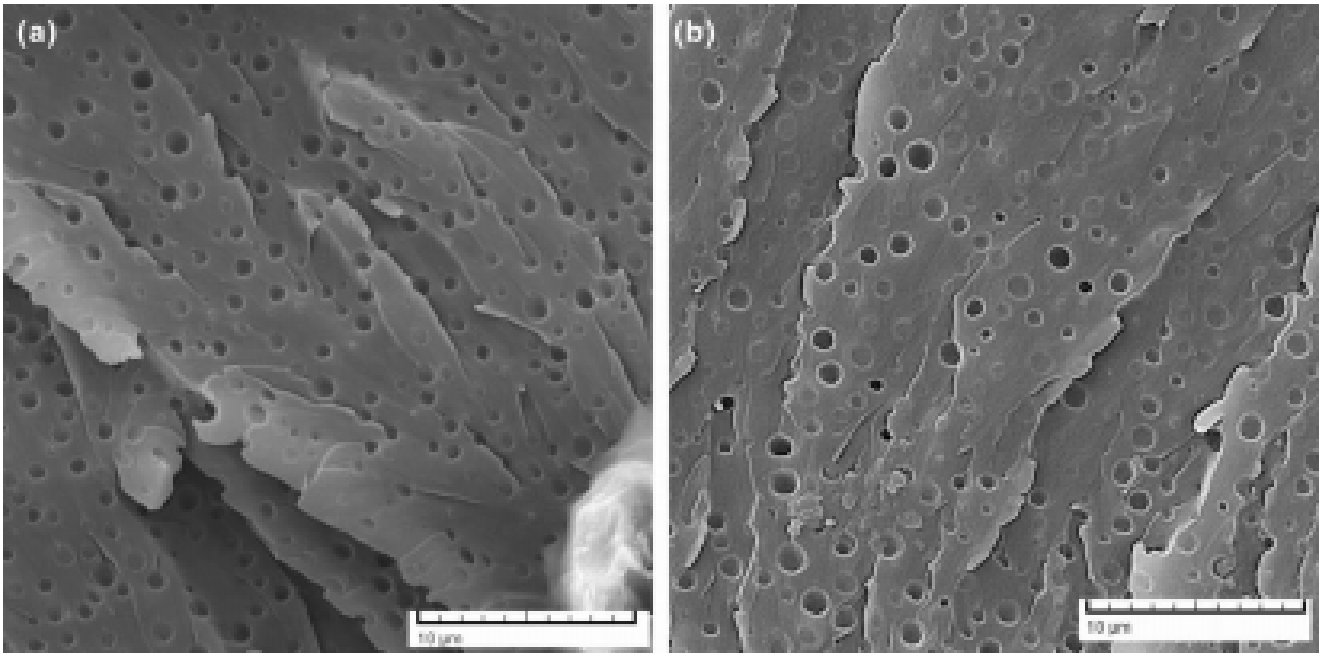

Figure 6 SEM photos taken from the damage surface of samples were tested at 50 mm/min: (a) A*10, (b) A10.

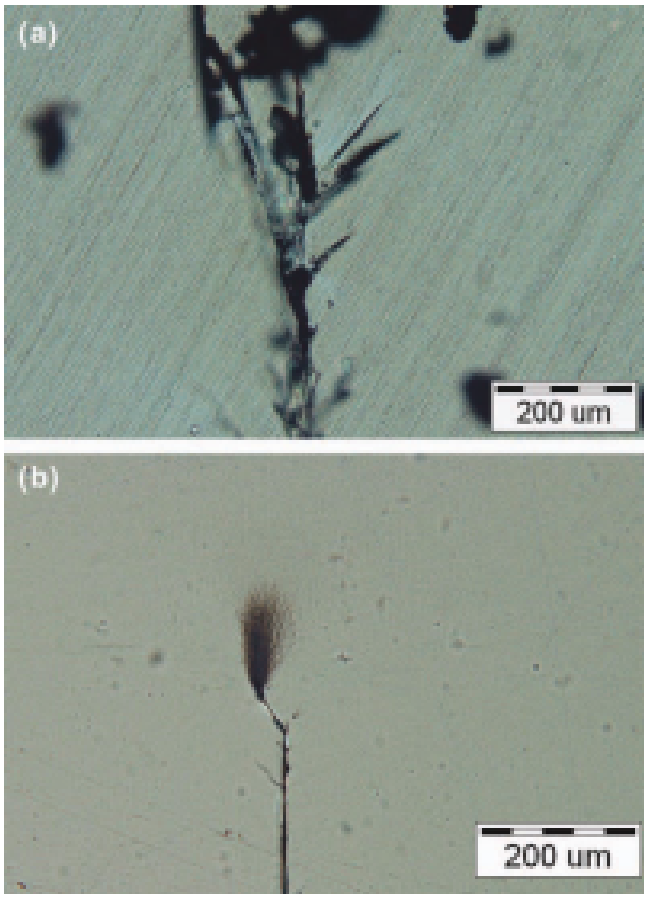

Figure 7 TOM photos of the midplane of the crack tip damage zone of samples tested at 50 mm/min: (a) A*10, (b) A10. [Color figure can be viewed in the online issue, which is available at wileyonlinelibrary.com].

toughness of modified epoxy may dramatically drop to the values close to that of neat resin because of suppression of toughening mechanisms at high loading rates.[13]

Similar trend is observed in the case of A10; the crack tip damage zone of A10 [Fig. 9(b)] shows very negligible shear yielding in the matrix. Note that tensile behavior of A10 specimens at 500 mm/min differs from those of 5 and 50 mm/min loading rates [Fig. 2(b)]. The lower fracture stress and strain with no evidence of plastic deformation corresponds to a brittle behavior of A10 which is similar to brittle behavior of A*10. Therefore, similar to A*10, it is expected that the K_{IC} of A10 reduces dramatically by increasing the loading rate.

In conclusion, while both modified blends behave brittle at the very high loading rate of 1000 mm/min, fracture behavior of A*10 is more sensitive to the loading rate at lower loading rates compared to that of A10. The following section tries to further analyze the concept of loading rate sensitivity in hybrid-modified epoxy.

Evidence in the literature

The literature survey performed revealed no similar study on the influence of loading rate on hybrid modified epoxies showing synergistic behavior. A rather old study by Kinloch et al.,[16] however, examined the influence of temperature on fracture toughness of a hybrid epoxy containing rubber particles and glass spheres. These investigators studied the fracture energy (G_{IC}) of a neat epoxy and a rubber-modified

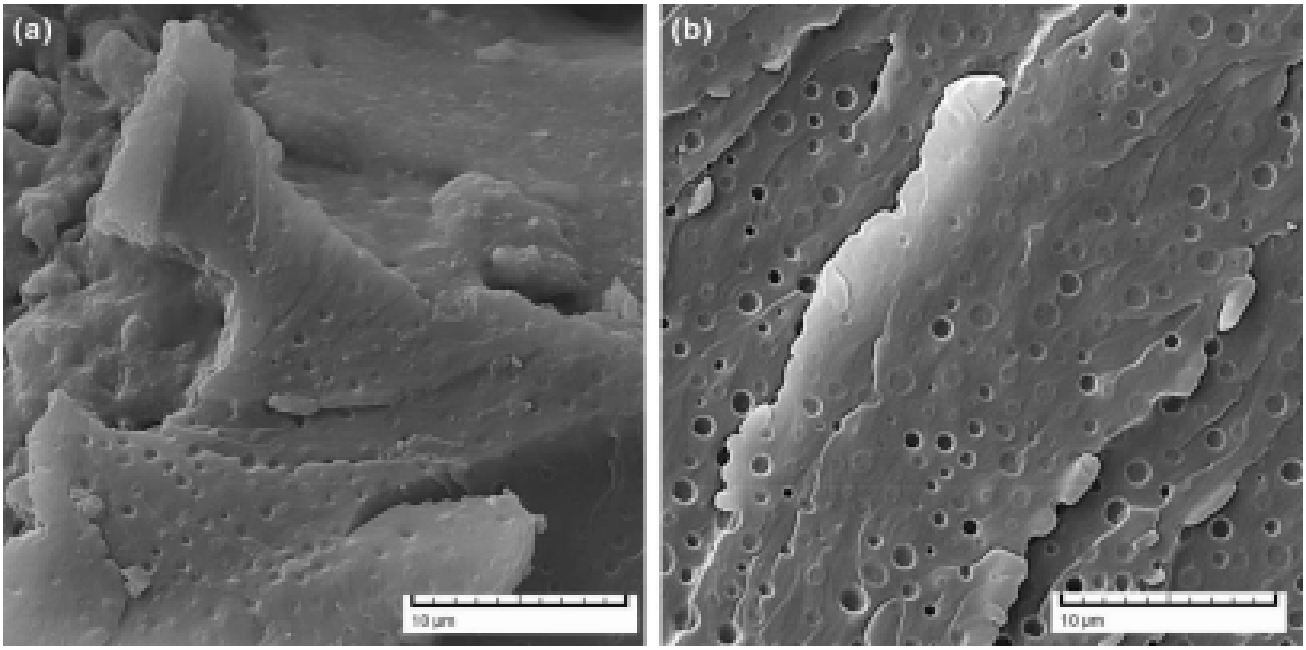

Figure 8 SEM photos taken from the damage surface of samples were tested at 500 mm/min: (a) A*10, and (b) A10.

epoxy containing 15 phr rubber at different temperatures while both systems were filled with different volume fractions of 50-μm glass beads. Although the synergistic toughening was not the main concern of this research, some of the formulations made by Kinloch et al.[16] resulted in extremely high values of fracture energy. To investigate the toughening mechanism in the hybrid systems, Kinloch et al.[16] conducted TOM study of the crack tip in some of their samples. Examination of their crack tips showed enlargement of the crack tip damage zone due to the interaction of the glass spheres with the crack tip stress field.[16]

Kinloch et al.,[16] observed that the fracture energy goes through a maximum by increasing the glass content at each temperature. The maximum level of fracture energy also declines significantly with decreasing the test temperature; there is almost no peak in −70°C test results. This observation illustrates that the toughening mechanism in their hybrid epoxy systems may be diminished by lowering the test temperature. Considering the time-temperature superposition principle in polymers, one may expect to see the same scenario if strain rate was increased instead of temperature rise.

This is similar to the finding of the current study that synergistic toughening was disappeared at high loading rates (Fig. 3). In other words, in a hybrid polymer blend synergistic toughening can be observed due to enlargement of damage zone.[13] However, increasing the loading rate or decreasing the temperature may suppress the enlargement of damage zone and thus, eliminate the synergistic

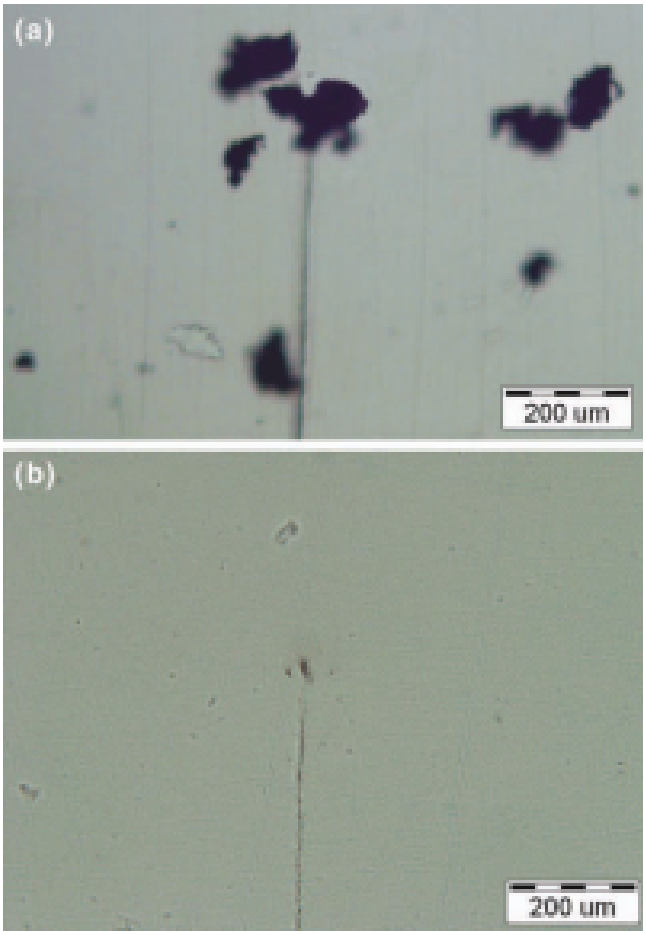

Figure 9 TOM photos of the midplane of the crack tip damage zone of samples tested at 500 mm/min: (a) A*10, (b) A10. [Color figure can be viewed in the online issue, which is available at wileyonlinelibrary.com].

toughening. Under these circumstances, the hybrid blend is no longer tougher than a simple rubber-modified blend (Fig. 3). Consequently, the hybrid blends showing synergistic toughening at ambient conditions may not be very much reliable at high strain rate or low temperature conditions. It seems that the sensitivity of the hybrid blends to the loading rate and temperature is more than those of simple rubber-modified blends. Further studies are needed to resolve these observations in rubber-modified polymers.

CONCLUSIONS

A DGEBA epoxy was toughened by 2.5 phr Tire and 7.5 phr ATBN rubber. At low rates of loading, synergistic toughening was observed, due to stretching the crack tip damage zone towards the Tire particles. However, at higher loading rates, this hybrid system showed lower K_{IC} than that of ATBN-modified (nonhybrid) resin with the same modifier content. TOM micrographs showed the toughening mechanism responsible for synergistic toughening was effectively suppressed with increasing the loading rate. Further, the crack resistance mechanisms of modified resins were almost eliminated, and the K_{IC} of the hybrid system decreased to the level of unmodified epoxy, at the loading rate of 1000 mm/min. These observations revealed that, despite the fact that hybrid system could produce higher K_{IC} than simple ATBN-modified epoxy at low loading rates; the synergistic toughening vanishes at high rates of loading. This means that the proposed hybrid modified epoxy is suitable for structures that are under semistatic loadings or low frequency fatigue conditions and do not experience high loading rates such as impact loading. Therefore, despite the superiority of the hybrid blend at low loading rate, a conventional nonhybrid rubber modified epoxy is preferred for high rates of loading.

The authors are thankful to Mr. Saeed Zokaee and Mr. Rasoul Lesan Khosh for their laboratory assistance.

References

1. Kinloch, A. J.; Shaw, S. J.; Tod, D. A.; Huntston, D. L. Polymer 1983, 24, 1341.
2. Pearson, R. A.; Yee, A. F. J Mater Sci 1991, 26, 3828.
3. Sue, H. J.; Garcia-Meitin, E. I.; Pickelman, D. M. In Polymer Toughening, Arends, C. B., Ed.; Marcel Dekker: New York, 1996; Chapter 5.
4. Yee, A. F.; Li, D. M.; Li, X. J Mater Sci 1993, 28, 6392.
5. Bagheri, R.; Pearson, R. A. J Mater Sci 1996, 31, 3945.
6. Bagheri, R.; Pearson, R. A. Polymer 1996, 37, 4529.
7. Bagheri, R.; Pearson, R. A. Polymer 2000, 41, 269.
8. DiBeradino, M. F.; Pearson, R. A.; In Toughening of Plastics Advances in Modeling and Experiments; Pearson, R. A.; Sue, H. J.; Yee, A. F., Eds.; ACS Symposium series no. 759: USA, 2000; Chapter 13.
9. Chen, T. K.; Jan, Y. H. J Mater Sci 1992, 27, 111.
10. Bagheri, R.; Williams, M. A.; Pearson, R. A. Polym Eng Sci 1997, 37, 245.
11. Abadyan, M.; Bagheri, R.; Kouchakzadeh, M. A. J Appl polym Sci, to appear.
12. Low, I. M.; Mai, Y. W. J Mater Sci 1989, 24, 1634.
13. Du, J.; Thouless, M. D.; Yee, A. F. Acta Mater 2000, 48, 3581.
14. Raghavan, D.; He, J.; Hunston, D.; Hoffman, D. J Adhes 2002, 78, 723.
15. Bucknall, C. B. In Polymer blends. II. Performance. Paul, D. R.; Bucknall, C. B., Eds.; Wiley: New York, 2000, Chapter 22.
16. Kinloch, A. J.; Maxwell, D. L.; Young, R. J. J Mater Sci 1985, 20, 4169.